NI

NASA Technical Memorandum 83206

CURRENT RESEARCH ON SHEAR BUCKLING AND THERMAL LOADS WITH PASCO: PANEL ANALYSIS AND SIZING CODE

(NASA-TM-83206) CURRENT RESEARCH ON SHEAR BUCKLING AND THERMAL LOADS WITH PASCO: PANEL ANALYSIS AND SIZING CODE (NASA) 13 p
HC A02/MF A01 CSCL 20K

N81-33501

Unclas
G3/39 27689

W. JEFFERSON STROUD, WILLIAM H. GREENE, AND MELVIN S. ANDERSON

SEPTEMBER 1981

NASA
National Aeronautics and Space Administration
Langley Research Center
Hampton, Virginia 23665

CURRENT RESEARCH ON SHEAR BUCKLING AND THERMAL LOADS WITH PASCO: PANEL ANALYSIS AND SIZING CODE

W. Jefferson Stroud
William H. Greene
Melvin S. Anderson

NASA Langley Research Center
Hampton, VA 23665

Summary

A computer program PASCO for obtaining the detailed dimensions of optimum (least mass) stiffened composite structural panels is described. Design requirements in terms of inequality constraints can be placed on buckling loads or vibration frequencies, lamina stresses and strains, and overall panel stiffness for each of many load conditions. General panel cross sections can be treated. In an earlier paper, PASCO was described and studies were presented which showed the importance of accounting for an overall bow-type imperfection when designing a panel--a capability available in PASCO. Since that paper, detailed studies have shown that the buckling analysis VIPASA in PASCO can be overly conservative for long-wavelength buckling when the loading involves shear. To alleviate that deficiency, an analysis procedure involving a smeared orthotropic solution was investigated. Studies are presented that illustrate the conservatism in the VIPASA solution and the danger in a smeared orthotropic solution. PASCO's capability to design for thermal loadings is also described. Design studies illustrate the importance of the multiple load condition capability when thermal loads are present.

Symbols

A	planform area of stiffened panel
B	panel width (see fig. 6)
E	Young's modulus
e	overall bow in panel, measured at midlength (see fig. 1)
G_{12}	shear modulus of composite material coordinate system defined by fiber direction
I	moment of inertia
L	panel length (see fig. 1)
M_x	applied bending moment per unit width of panel (see fig. 1)
N_x, N_y, N_{xy}	applied longitudinal compression, transverse compression, and shear loading, respectively, per unit width of panel (see fig. 1)
N_{x_E}	Euler buckling of panel - buckling load for $\lambda = L$
P	lateral pressure
S	area of panel cross section
u,v,w	buckling displacements
W	mass of stiffened panel
$\frac{W/A}{L}$	mass index
X,Y,Z	coordinate axes
x,y,z	coordinates
α	coefficient of thermal expansion
γ	N_x/N_{x_E}
ΔT	change in temperature
λ	buckling half-wavelength
μ_1, μ_2	Poisson's ratios of composite material in coordinate system defined by fiber direction, $\mu_2 = \mu_1 E_2/E_1$
ρ	density
σ	stress

Subscripts

1	fiber direction
2	normal to fiber direction
i	integer associated with plate element i

Introduction

The introduction of composite materials has greatly expanded the options for obtaining efficient structural designs. Because of the large number of design options, the task of finding the optimum configuration for a composite structure is more difficult than for the corresponding metal structure. This opportunity to obtain superior designs together with the difficulty of selecting among many options is making automated structural sizing an increasingly attractive design tool. Not only do composite materials provide an increase in the number of design variables, they can also cause an increase in the complexity of the failure modes. Rules of thumb that prevent undesirable proportions for metal structures are often inadequate for the corresponding composite structure. For that reason, the automated structural sizing procedure must incorporate accurate structural analysis methods. For stiffened composite structural panels, a computer program denoted PASCO (Panel Analysis and Sizing COde) has been developed and described in references 1-4. PASCO includes both the generality necessary to exploit the added design flexibility afforded by composite materials and an accurate buckling analysis--VIPASA[5] (Vibration and Instability of Plate Assemblies including Shear and Anisotropy)--to detect and account for complex buckling modes. PASCO can design for buckling, frequency, material strength and panel stiffness requirements. An important limitation of PASCO is that VIPASA underestimates the buckling load for long wavelength buckling when the

loading involves shear.

This paper is divided roughly into three parts. In the first part, the capabilities of and approach used in PASCO are described briefly. In the second part, the conservatism in VIPASA for long-wavelength shear buckling is explained and illustrated. To alleviate that deficiency, an alternate analysis procedure based on a smeared orthotropic solution was investigated. Calculations are presented which show the danger in using that solution. In the third part, PASCO's capability to design for thermal loadings is described. Design studies illustrate the importance of the multiple load condition capability when thermal loads are present.

Description of PASCO

PASCO is described in detail in references 1-4; therefore, the description presented here is a summary.

Capabilities

PASCO has been designed to have sufficient generality in terms of panel configuration, loading, and practical constraints so that it can be used for sizing of panels in a realistic design application. The panel may have an arbitrary cross section composed of an assembly of plate elements with each plate element consisting of a balanced symmetric laminate of any number of layers. The panel cross section, material properties, loading, and temperature change are assumed to be uniform in the X direction (fig. 1). Any group of dimensions, including ply angles, may be selected as design variables; the remaining dimensions can be held fixed or related linearly to the design variables.

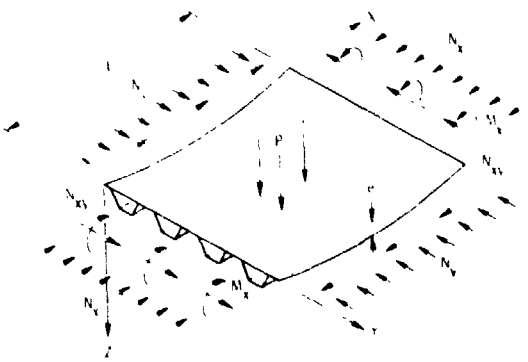

Figure 1.- Stiffened panel with initial bow, applied loading, and coordinate system.

The panel may be loaded by any combination of in-plane loadings (tension, compression, and shear) and lateral pressure as indicated in figure 1. Multiple load conditions can be treated. Thermal stresses resulting from temperature changes are calculated. The material properties corresponding to the temperature of each plate element may be changed for different load cases. The effect of an overall panel imperfection e, shown in figure 1, can also be taken into account. One of the improvements that has been made to the code since reference 1 is that an overall bending moment M_X, shown in figure 1, can be accounted for in an approximate manner.

Realistic design constraints such as minimum ply thickness, fixed stiffener spacing, upper and/or lower bounds on extensional and shear stiffness may be prescribed. The vibration frequency of the panel (including the effect of prestress) may be specified to exceed a given value. Buckling loads and vibration frequencies are calculated by the VIPASA computer program.[5] Stresses and strains in each layer of each plate element are calculated and margins against material failure are calculated based on an assumed material strength failure criterion.

Optimization Approach

A nonlinear mathematical programming approach with inequality constraints is used to perform the optimization. The optimizer is CONMIN.[6,7]

Sizing variables.- The sizing variables (design variables) are the widths of the plate elements that make up the panel cross section, the ply thicknesses, and the ply orientation angles. Any set of widths, thicknesses and orientation angles can be selected as the active sizing variables. The remaining widths, thicknesses, and orientation angles can be held fixed or linked linearly to the active sizing variables. Upper and lower bounds can be specified.

Objective function.- The objective function is the panel mass index W/L, the panel mass per unit area divided by the panel length. The panel length is fixed; therefore, the quantity that is minimized is the panel mass per unit width.

Constraints.- Inequality constraints can be placed on buckling loads or vibration frequencies (loaded or unloaded), lamina stresses or strains (material strength constraints), and panel stiffness. These constraints can be applied for each of many load conditions.

For the buckling and vibration constraints, separate constraints are applied for each wavelength. With this approach, panels can be designed with a different margin of safety for each wavelength. Constraints can also be placed on several eigenvalues at the same wavelength.

For the material strength constraints, three strength criteria are available in PASCO: maximum lamina stress, maximum lamina mechanical strain, and the Tsai-Wu criterion[8]. For the maximum stress criterion, tension and compression limits are placed on lamina stresses in the fiber direction and transverse to the fiber direction. Limits are also placed on the shear stress. The maximum lamina mechanical strain criterion is defined similarly, except that the thermal strain is subtracted from the total strain to provide the mechanical strain. The Tsai-Wu criterion involves a quadratic function of the stresses. Failure is assumed to occur when the stress state in any lamina exceeds the failure criterion.

For the stiffness constraints, upper or lower bounds can be placed on the extensional stiffness, the shear stiffness, and the bending stiffness. These stiffnesses are "smeared" orthotropic stiffnesses for the overall panel, not individual plate element stiffnesses. The extensional stiffness is associatd with the N_X load, the shear stiffness with the N_{XY} load, and the bending stiffness with the M_X load. These loads are shown in figure 1.

Constraint Approximation.- A constraint approximation approach[9] is used in PASCO to increase the computational efficiency when the program is used for sizing. That approach is depicted schematically in

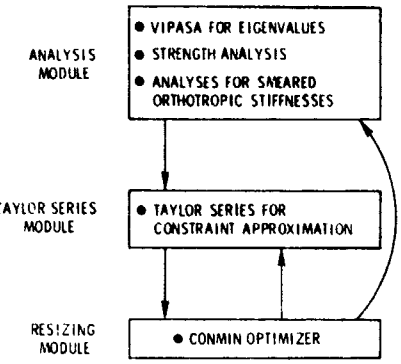

Figure 2.- General sizing approach used in PASCO.

figure 2. In the analysis module, all constraints are calculated with VIPASA and supporting subroutines. The program identifies the critical constraints and, using finite difference approximations, calculates derivatives of the critical constraints with respect to the sizing variables. These derivatives are then passed to the Taylor series module which generates a first order Taylor series expansion of each constraint. These expansions provide the approximate constraints for CONMIN. CONMIN interacts only with these approximate explicit functions that represent the contraints, not with VIPASA.

The design strategy consists of a series of sizing cycles in which CONMIN adjusts the values of the sizing variables based on approximate values of the constraints. An upper limit is imposed on the change of each sizing variable during each sizing cycle. The end point of one sizing cycle becomes the initial point of the next sizing cycle. Accurate values of the constraints and derivatives of the constraints are then recalculated, and new Taylor series expansions are generated. Ten sizing cycles are usually adequate to obtain convergence if the initial design is reasonably well chosen.

Shear Buckling Problem

As is pointed out earlier in this paper, an important limitation of PASCO is that VIPASA underestimates the buckling load when the loading involves shear and the buckle mode is a general or overall mode in which a single half wave extends from one end of the panel to the other. That shortcoming is explored in this section.

VIPASA Buckling Analysis

VIPASA, the buckling analysis program incorporated in PASCO, treats an arbitrary assemblage of plate elements with each plate element i loaded by N_{x_i}, N_{y_i}, and N_{xy_i}. The buckling analysis connects the individual plate elements and maintains continuity of the buckle pattern across the intersection of neighboring plate elements. The buckling displacement w assumed in VIPASA for each plate element is of the form

$$w = f_1(y)\cos\frac{\pi x}{\lambda} - f_2(y)\sin\frac{\pi x}{\lambda} \qquad (1)$$

Similar expressions are assumed for the inplane displacements u and v. The functions $f_1(y)$ and $f_2(y)$ allow various boundary conditions to be prescribed on the lateral edges of the panel. Boundary conditions cannot be prescribed on the ends of the panel.

For orthotropic plate elements with no shear loading, $f_2(y)$ is zero. The solution $f_1(y)\cos\frac{\pi x}{\lambda}$ gives a series of node lines that are straight, perpendicular to the longitudinal panel axis, and spaced λ apart as shown in figure 3. Along each of these node lines, the buckling displacements satisfy simple support boundary conditions. For values of λ given by $\lambda = L, L/2, L/3, \ldots L/m$, where m is an integer, the nodal pattern shown in figure 3 satisfies simple support boundary conditions at the ends of a finite, rectangular, stiffened panel of length L.

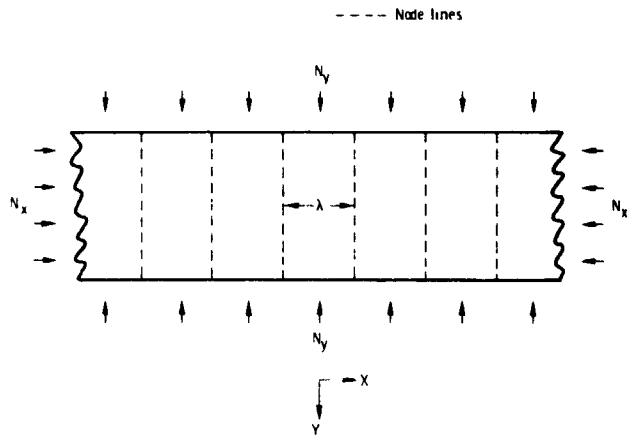

Figure 3.- Node lines produced by $w = f_1(y)\cos\frac{\pi x}{\lambda}$

For anisotropic plate elements and/or plate elements with a shear loading, $f_2(y)$ is not zero. (Because anisotropy generally has negligible effect for long wavelength buckling modes and because it is these long wavelength modes that are troublesome, reference to anisotropy is dropped in the following discussion). Node lines are skewed and not straight, but the node lines are still spaced λ apart as shown in figure 4. Since node lines cannot coincide with

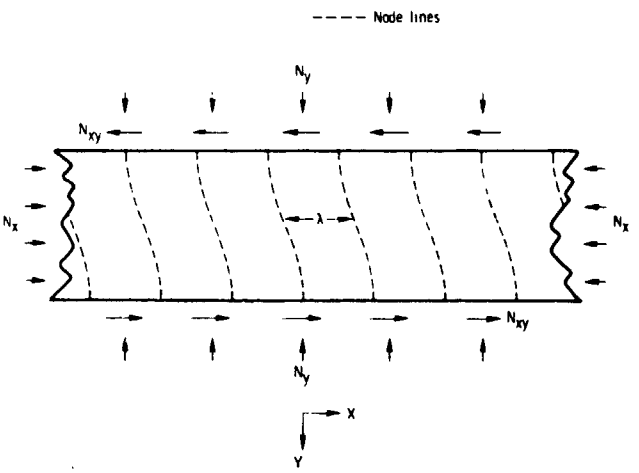

Figure 4.- Node lines produced by $w = f_1(y)\cos\frac{\pi x}{\lambda} - f_2(y)\sin\frac{\pi x}{\lambda}$

the ends of the rectangular panel, the VIPASA solution for loadings involving shear is accurate only when many buckles form along the panel length, in which case boundary conditions at the ends are not important. An example in which $\lambda = L/4$ is shown in figure 5.

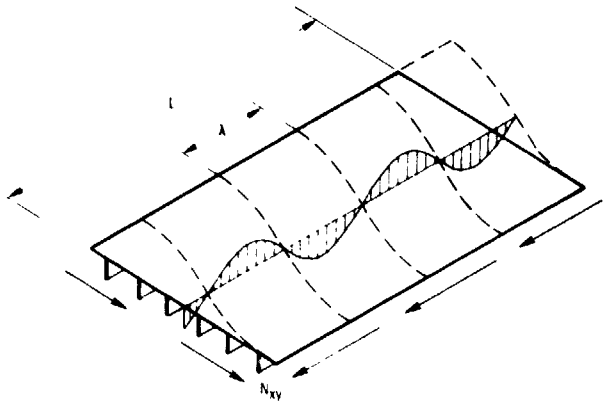

Figure 5.- Buckling of panel under shear loading. Mode shown is $\lambda = L/4$.

As λ approaches L, the VIPASA buckling anaylsis for a panel loaded by N_{xy} may underestimate the buckling load substantially. One explanation is as follows: As seen in figure 5, the skewed nodal lines given by VIPASA in the case of shear do not coincide with the end edges. Forcing node lines (and, therefore, simple support boundary conditions) to coincide with the end edges produces long-wavelength buckling loads that are, in many cases, appreciably higher than those determined by VIPASA.

In summary, for stiffened panels composed of orthotropic plate elements with no shear loading, the VIPASA solution is exact in the sense that it is the exact solution of the plate equations satisfying the Kirchoff-Love hypothesis. However, for stiffened panels having a shear loading the VIPASA solution can be very conservative for the case $\lambda = L$.

Because VIPASA is overly conservative in the case of long-wavelength buckling if a shear load is present, other easily-adaptable analysis procedures based on smeared orthotropic stiffnesses have been explored for the case $\lambda = L$.

Smeared Stiffener Solution

The objective of the analysis is to solve the shear buckling problem for the finite panel illustrated in figure 6. For buckling half-wavelength λ equal to panel length L, the mathematical model solved by VIPASA and the resulting node lines are similar to those illustrated in figure 7. The panel in figure 7 is infinitely long in the X direction.

It is assumed that a better approximation to the solution for the finite panel would be obtained with the infinitely wide panel shown in figure 8. Unfortunately, the mathematical model illustrated in figure 8 cannot be analyzed with VIPASA because VIPASA requires that the panel be uniform in the direction of the infinite dimension. However, the mathematical model obtained by smearing the stiffnesses of the stiffened panel of figure 8 can be analyzed with VIPASA. That solution is referred to as the smeared stiffener solution. It is obtained by interchanging the x and y loading and stiffnesses. The eigenvalue used is the lowest of the set for $\lambda = B, B/2, B/3, \ldots$ where B is the panel width. (The attempt to improve on the VIPASA solution for long-wavelength shear buckling is more involved than the discussion presented here. However,

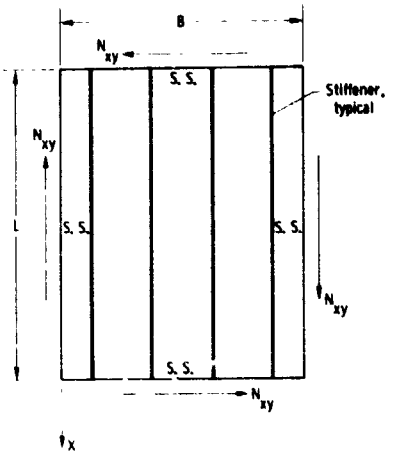

Figure 6.- Finite stiffened panel of length L and width B, simply supported on all four edges, and subjected to shear load N_{xy}.

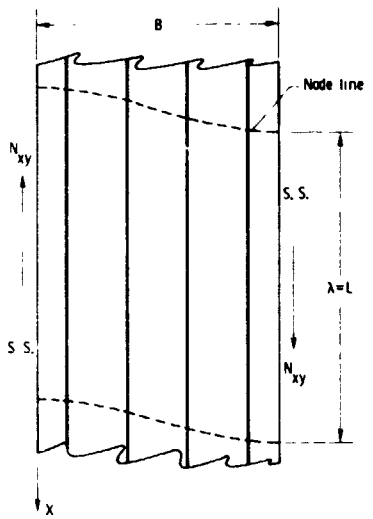

Figure 7.- Node lines given by VIPASA for shear buckling with $\lambda = L$.

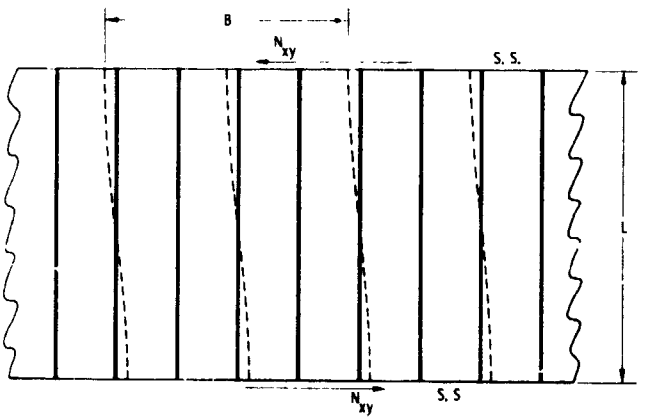

Figure 8.- Node lines for buckling of infinitely-wide stiffened panel.

the basic feature--smeared stiffener solution--of that solution approach and the conclusions regarding its suitability are the same as those presented here. A more complete discussion is presented in references 2 and 4).

Examples

Two stiffened panels were analyzed with PASCO and with the general finite element structural analysis code EAL (refs. 10, 11) to assess the validity of the VIPASA analysis for long wavelength shear buckling and the smeared stiffener solution. Both panels had six equally-spaced blade stiffeners, were 76.2 cm (30 in.) square, and were made of a graphite-epoxy composite material having the material properties given in table I. The loadings were combinations of longitudinal compression (N_x) and shear (N_{xy}). A schematic drawing showing the loading and overall dimensions for the example cases is shown in figure 9. The manner in which the applied loads were distributed over the cross section--the prebuckling stress state--is discussed in reference 2. In particular, the N_x load was distributed assuming uniform strain ϵ_x of the panel cross section with free transverse expansion of each plate element, so that N_{y_i} was zero. Buckling boundary conditions were simple support on all four edges. These boundary conditions are defined in figure 9. The panel cross sections were treated as collections of lines with no offsets to account for thicknesses. (Offsets are available in PASCO). The first example is discussed in greater detail than the second example.

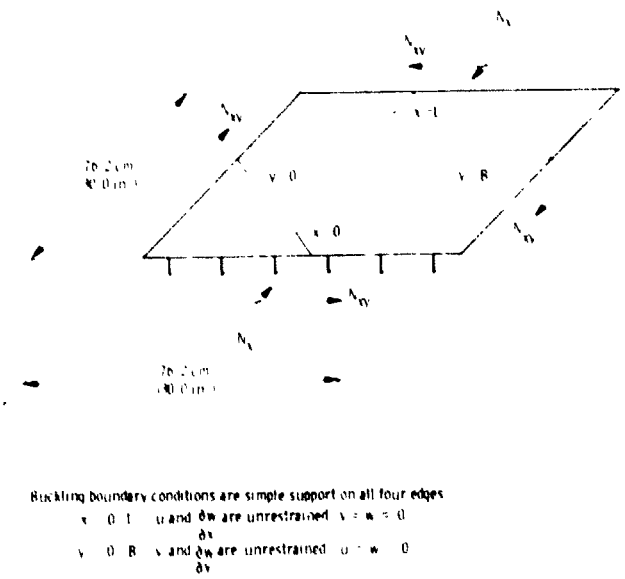

Figure 9.- Loading, dimensions, and boundary conditions for stiffened panel examples.

Example 1.- A repeating element of the composite blade-stiffened panel is shown in figure 10. Element widths are also shown. The wall construction for each plate element is given in table II. Only half the laminate is defined for each plate element because all laminates are symmetric. Plate element numbers are indicated by the circled numbers in figure 10. Fiber orientation angles are measured with respect to the X axis, which is parallel to the stiffener direction.

The single finite element type used in the EAL model for this and the other example is a four-node, quadrilateral, combined membrane and bending element. Both the membrane and bending stiffness matrices for the element are based on the assumed stress, hybrid

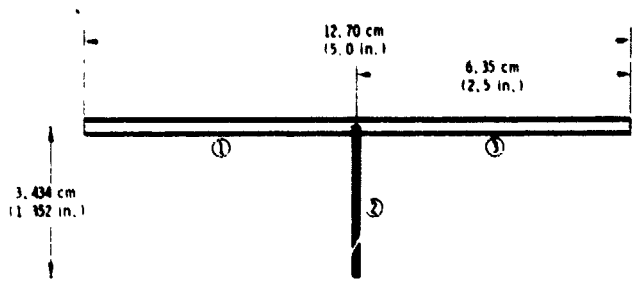

Figure 10.- Repeating element for example 1, composite blade-stiffened panel.

formulation of the Pian type.[10,12] The buckling or geometric stiffness matrix for the element is based on a conventional displacement formulation that includes terms allowing inplane (u and v displacements) as well as out-of-plane (w displacements) buckling modes. The Pian membrane formulation allows a single element across the depth of a blade stiffener to accurately represent its overall inplane bending behavior. The EAL designation for this element is E43. The finite element grid chosen for the EAL model is shown in figure 11. Two elements are used along the depth of the blade, four elements are used between blades, and 36 elements are used along the length, making a total of 1296 elements, and 1369 nodes. Based on convergence studies and other comparisons, it is believed that the finite element calculations presented in this paper differ from the exact solution by no more than approximately one percent and, therefore, provide benchmark calculations.

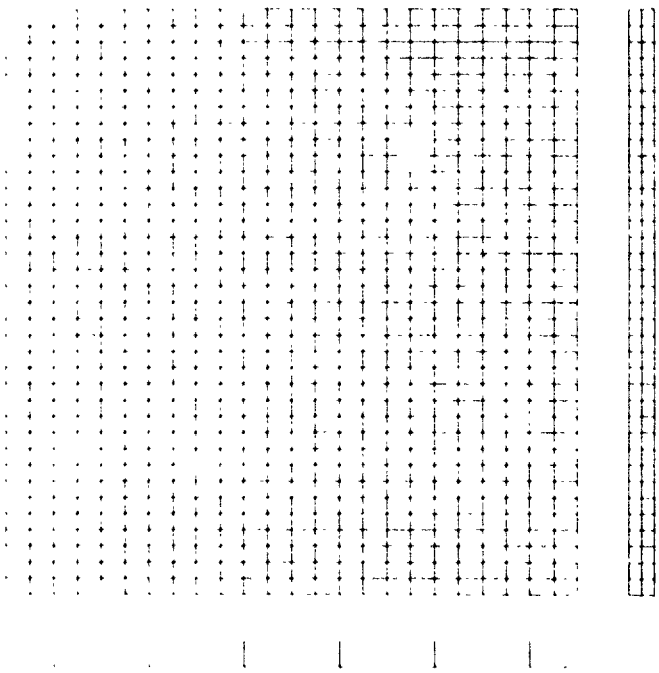

Figure 11.- EAL finite element model for example 1, composite blade-stiffened panel.

Buckling results are shown in figure 12. The curves indicate VIPASA and smeared stiffener solutions, and the circular symbols indicate EAL solutions. The solid curve represents the VIPASA solution for buckling half-wavelength λ equal to L. The dotted line at

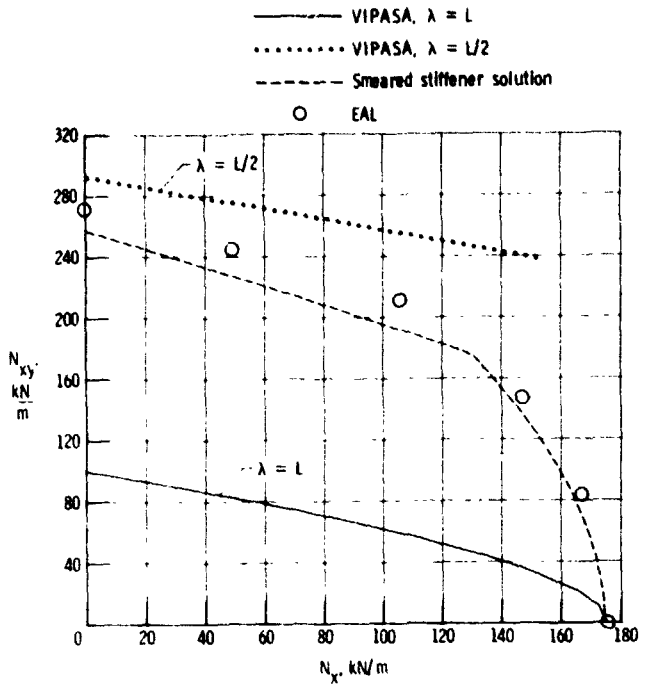

Figure 12.- Buckling load interaction for example 1, composite blade-stiffened panel.

the top of the figure represents the VIPASA solution for λ equal to L/2. The dashed curve represents the smeared stiffener solution and indicates solutions for the lowest buckling load of the set λ = B, B/2, B/3,.... where B is the panel width. The corner in the dashed curve that occurs at N_x equal to approximately 130 kN/m (750 lb/in) indicates a change in mode shape for the smeared stiffener solution. For N_x less than 130 kN/m, the buckling half-wavelength transverse to the stiffeners is equal to 38 cm (15 in.) which is three times the stiffener spacing. For N_x greater than 130 kN/m, the buckling half-wavelength transverse to the stiffeners is equal to 76 cm (30 in.) which is six times the stiffener spacing.

For this example, the smeared stiffener solution gives reasonably accurate estimates of the solution for all combinations of N_x and N_{xy}. For the loading N_x = 0, the smeared stiffener solution is about five percent lower than the EAL solution. For this same loading, the VIPASA solution for λ = L is about 63 percent lower than the EAL solution. For the loading N_{xy} = 0, the VIPASA solution for λ = L and the EAL solution agree to within 0.3 percent.

Detailed comparisons and benchmark calculations for six loadings are presented in table III. In this table, the quantity denoted FACTOR is the solution in terms of a scale factor for the specified loading. For example, for the loading N_x = 350.3 kN/m, N_{xy} = 175.1 kN/m (N_x = 2000 lb/in, N_{xy} = 1000 lb/in) the EAL solution of FACTOR = 0.4764 means that the solution is N_x = 0.4764 x 350.3 = 166.9 kN/m (952.8 lb/in) N_{xy} = 0.4764 x 175.1 = 83.37 kN/m (476.4 lb/in).

Finally, the buckling mode shape obtained with EAL for the case N_x = 0 is shown in figure 13. This contour plot of the buckling displacement w shows that the buckling half-wavelength transverse to stiffeners is approximately equal to three times the stiffener spacing, which was predicted by the smeared stiffener solution.

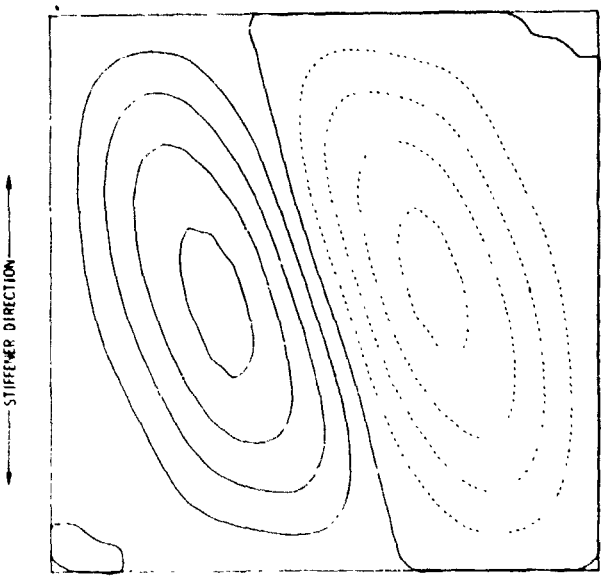

Figure 13.- Shear buckling mode shape obtained with EAL for example 1, composite blade-stiffened panel.

Example 2.- A repeating element of a heavily-loaded composite blade-stiffened panel is shown in figure 14. The wall construction for each plate element is given in table IV.

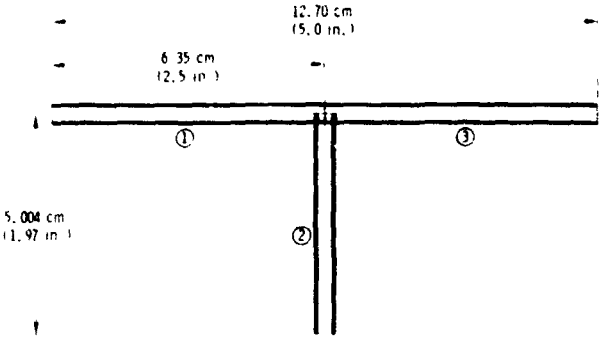

Figure 14.- Repeating element for example 2, heavily loaded, composite blade-stiffened panel.

Buckling solutions for example 2 are shown in figure 15. The solid curve indicates the VIPASA solution for λ = L. The dotted curves indicate VIPASA solutions for λ = L/2, L/4, and L/5. The dashed curve represents the smeared stiffener solution. As in the first example, the corners in the dashed curve indicate changes in mode shape. For N_x less than about 700 kN/m (4000 lb/in) the buckling half-wavelength transverse to the stiffeners is 1.5 times the stiffener spacing. For N_x greater than about 700 kN/m but less than about 1600 kN/m (9000 lb/in) the buckling half-wavelength transverse to the stiffeners is 2.0 times the stiffener spacing. For N_x greater than about 1600 kN/m but less than about 1800 kN/m, the buckling half-wavelength transverse to the stiffeners is 3.0 times the stiffener spacing.

For this example, the EAL results fall below both the smeared stiffener solution and the λ = L/2, L/4, and L/5 curves. For the N_x = 0 case, an examination of the EAL buckling mode shape presented in figure 16 shows that the lowest buckling load is an overall mode (λ = L) rather than a λ = L/2 mode, which might

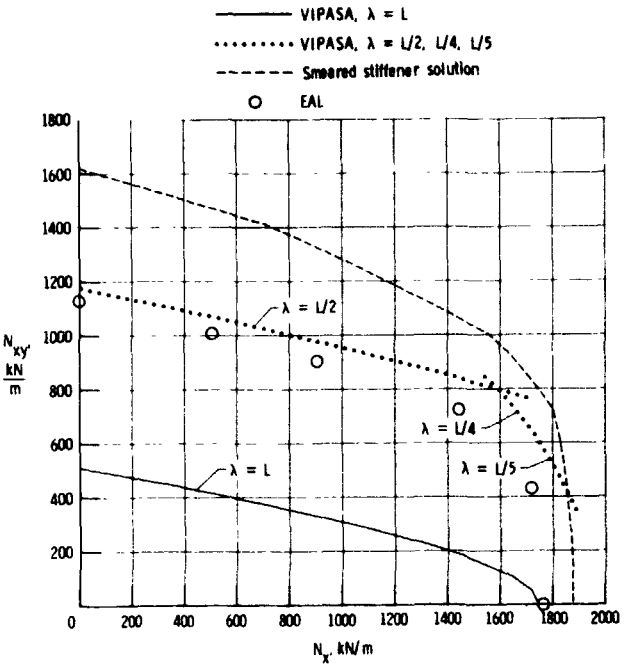

Figure 15.- Buckling load interaction for example 2, heavily-loaded, composite blade-stiffened panel.

have been assumed since the λ = L/2 solution is near the EAL solution. Detailed comparisons of solutions for six loadings are presented in table V.

Discussion of results.- The basic conclusion that can be drawn from these calculations and from similar results presented in reference 4 is that a buckling solution based on smearing the overall stiffnesses of a stiffened panel should be used only with caution.

In the first example, the smeared stiffener solution underestimated the overall buckling load slightly. In the second example, it greatly overestimated the overall buckling load. One factor that appeared to contribute to the error in the second example was that the buckle half-wavelength transverse to the stiffeners was only 1.5 times the stiffener spacing. Usually, that short a wavelength invalidates the stiffness smearing approach. In PASCO, the smeared stiffener solution should not be accepted if the buckle half-wavelength transverse to the stiffeners is less than 2.5 times the stiffener spacing.

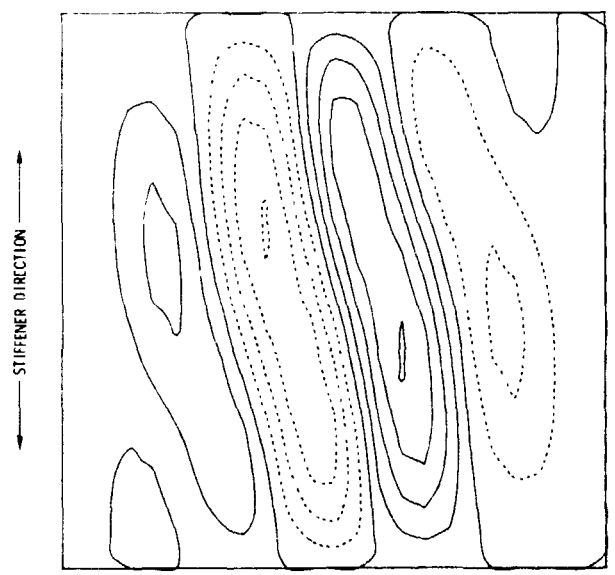

Figure 16.- Shear buckling mode shape obtained with EAL for example 2, heavily-loaded, composite blade-stiffened panel.

Because an automated design procedure generally exploits a defect in an analysis, it is recommended that the smeared stiffener approach not be used in sizing applications. The panels designed using the standard VIPASA analysis will be light-weight and conservatively designed.

In all cases, the finite element solution for overall buckling falls between the VIPASA solutions for λ = L and λ = L/2. A solution approach for overall shear buckling that assumes the buckling mode to be a combination of the first few VIPASA modes is being studied. A special procedure is needed to combine these modes in such a way that the boundary conditions at the panel ends are satisfied.

Thermal Loads In Panel Design

The PASCO program can perform a simplified thermal stress analysis, add the stress resultants due to the temperature effects to those obtained from other loadings and then determine the buckling load of the panel. A brief summary of this analysis will be given followed by design studies that illustrate how temperature and thermal stress can be treated in PASCO.

Thermal Stress Anaysis

In PASCO, a basic assumption in the buckling analysis is that all structural quantities and loadings are constant along the length. Therefore, temperatures must be assumed constant along the length, and any stress distribution determined as being representative of the stress distribution in the center of the panel is also assumed constant along the length. Temperature may vary along the width and depth direction of the panel but is constant through the thickness of a given wall cross-section. The temperature distribution is prescribed; it does not change as the sizing variables are changed.

The classical equation for thermal stress in a beam is the basis of the analysis

$$\sigma = \alpha E \Delta T - \frac{1}{S}\int_S \alpha E \Delta T \, dS - \underline{\frac{z}{I}\int_S \alpha E \Delta T z \, dS} \qquad (2)$$

This equation suitably modified to account for orthotropic laminate properties (as shown in detail in ref. 2) is used in two different ways in PASCO. Consider a panel over many supports as illustrated in figure 17. The behavior of an individual bay would depend on its location. In the end bay, the stress distribution predicted by equation (2) would develop. The end bay would also have a bow produced by the bending moment generated by the underlined term. If there were an axial load N_x as well, this bow and the bending stresses produced by the bow would be increased by the

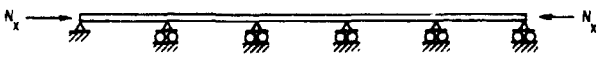

Figure 17.- Panel over many supports.

ratio $1/(1-\gamma)$, the beam-column effect. All these effects are included in PASCO when a parameter ITHERM is set equal to 1.

In the center of the panel, any tendency to bow would be restrained by adjacent bays and the stress distribution would be given by equation (2) with the underlined term omitted. In this case, there would be no bow due to thermal stress. This stress analysis is performed when the parameter ITHERM is set to zero.

When designing a panel subject to temperature, it is customary to require that the load also be sustained without temperature. In addition, if the panel spans many supports and if the same detailed dimensions are to be used for both end bays and interior bays, then the panel must be designed to carry the load with and without the thermal bow. The result is a multiple load condition problem. Such design problems are illustrated in the following examples.

Examples

Design requirements.- Several example studies were carried out to determine the effect on panel mass of design requirements involving temperature change. All studies used the overall dimensions, basic configuration, and stacking sequence of the blade-stiffened panels used in the shear buckling studies. Three types of studies are presented. In the first study, panels were made of a graphite-epoxy material having the properties given in table I. Sizing variables were the depth of the blade and the thicknesses of the plies; ply angles were fixed. The second study was similar to the first, except that ply angles were added to the sizing variables. In the third study, panels were made of aluminum. The importance of the thermal bow and the importance of the multiple load condition capability are demonstrated.

To provide for the bending loads that occur when the panel is allowed to take on a thermal bow, the blade portion of the stiffened panel was divided into seven sections as shown in figure 18. (The load N_{x_i} in each plate element i is uniform). The tip element of the blade was made very small so that prebuckling strains could be calculated accurately near the tip of the blade. These strains were monitored and used in the material strength criterion that is based on maximum mechanical strain. The normal strains were required to be less than 0.004, and the shear strain less than 0.01.

The following five load conditions were used:

Load Condition	N_x, kN/m (Compression)	Thermal Bow	Temperature Change, ΔT, ^oK
1	175.1	No	-111.1
2	175.1	No	Variable
3	175.1	No	0
4	175.1	Yes	Variable
5	175.1	Yes	-111.1

The loading 175.1 kN/m corresponds to 1000 lb/in, and the temperature change -111.1^oK corresponds to -200^oF. Temperature changes are measured with respect to the temperature for a zero residual stress state in the composite material. Normally, this reference temperature is higher than room temperature. The three design temperature changes then correspond to a uniform cold condition ($\Delta T = -111.1^oK$), a transition condition in which the skin is hot and the tip of the blade is cold (variable), and a uniform hot condition ($\Delta T = 0^o$). In the transition condition (variable), the temperature

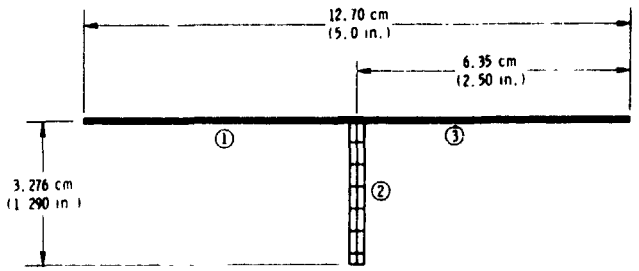

Figure 18.- Repeating element for graphite-epoxy panel designed for load conditions 1 to 5.

change in each element is as follows: skin, 0^oK; first element in blade (adjacent to skin), -36.1^oK; second element, -66.7^oK; third to seventh elements are -86.1^oK, -97.2^oK, -105.5^oK, -108.3^oK, -111.1^oK.

Graphite-epoxy panels, fixed ply angle.- Results of the design study for the graphite-epoxy blade-stiffened panel with fixed ply angles are presented in table VI. The first column (far left) indicates the load conditions used to obtain a design. For example, the third entry in that column indicates load conditions 1, 2, and 3. The second column is the mass index $\frac{W/A}{L}$ of the minimum mass panel that supports that combination of load conditions. The final five columns are the ratios of the lowest buckling load to the design loading for each of the five loading conditions. The ratios are applied to both the compressive load and the change in temperature.

The data in the first row shows that a panel designed for a temperature change (load condition 1) need not carry the load when the temperature is removed (load condition 3). The panel designed for load conditions 3, 4, and 5 is the same as the panel designed for all five load conditions. The dimensions of the repeating element for that panel are shown in figure 18. Thicknesses are given in table VII. The skin consists of $+45^o$ plies only; the blade consists of 0^o and $\pm 45^o$ plies only.

Graphite-epoxy panels, variable ply angle.- In two panels, ply angles were allowed to vary. Each panel was designed to carry load conditions 1 to 5. In the first panel, only the angles in the skin were varied. The result was that the skin of the final design consisted only of $\pm 58.2^o$ plys and the mass index was reduced 6% to 4.052 kg/m^3. In the second panel, the angles of the plys originally at $\pm 45^o$ in both the skin and the blade and the angles of the plys originally at 0^o in the blade were varied. The additional mass reduction was negligible.

Aluminum panels.- Design studies similar to those presented in table VI for graphite-epoxy panels were also carried out for aluminum panels having the material properties given in table VIII. Results are presented in table IX. Since uniform temperature changes produce no thermal stress for these panels, the original five loading conditions reduce to three: 1, 2, and 4. The repeating element for the panel that supports all three loads is shown in figure 19.

Discussion of results.- Three conclusions can be drawn from these calculations. First, when design requirements involve thermal loads it is advisable to use a multiple load condition approach with various temperature distributions and end support conditions. For the examples presented in this paper, the increase in

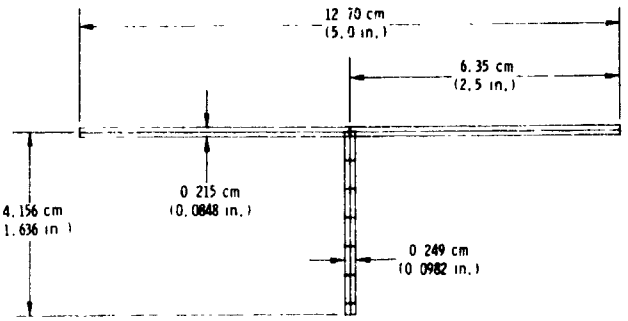

Figure 19.- Repeating element for aluminum panel designed for load conditions 1, 2, and 4.

panel mass caused by using this approach is small compared to the increase in load carrying ability for off-design load conditions that may be encountered in service. This is true whether the panel is graphite-epoxy or aluminum.

The second conclusion is that it is more important to use the multiple load condition capability for composite panels than for metal panels. The increase in the number of design variables provided by composite materials allows a composite structure to be tailored very well to a specific load condition. However, this highly tailored structure may have very little load carrying ability for off-design conditions. This point is illustrated in reference 13 for the case of damage tolerance in wing structures.

The third conclusion is that ply angle variation can provide a moderate (6%) reduction in mass even in a five-load-condition-design.

Concluding Remarks

A computer program denoted PASCO for obtaining the dimensions of optimum (least mass) stiffened composite structural panels is described. The capabilities of and approach used in PASCO are discussed briefly.

PASCO's buckling analysis (VIPASA) is reviewed, and an important shortcoming of that analysis--underestimation of long wavelength shear buckling loads--is explained. Studies involving combined longitudinal compression and shear loadings are presented to demonstrate VIPASA's conservatism for long-wavelength shear buckling. It is shown that an easily adaptable smeared orthotropic solution may be unconservative for predicting long-wavelength shear buckling. Therefore, it is recommended that the smeared solution not be used for sizing applications.

Studies also demonstrate the capability in PASCO to design for thermal stresses, to account for multiple loading conditions, and to use ply angles as sizing variables. The importance of using the multiple load condition capability for thermal loadings is illustrated for both graphite-epoxy and aluminum panels. Ply angle variation provided a 6% mass reduction for a multiple load condition case.

References

1. Anderson, Melvin S.; and Stroud, W. Jefferson: A General Panel Sizing Computer Code and Its Application to Composite Structural Panels. AIAA J., Vol. 17, No. 8, August 1979, pp. 892-897.

2. Stroud, W. Jefferson; and Anderson, Melvin S.: PASCO: Structural Panel Analysis and Sizing Code, Capabilty and Analytical Foundations. NASA TM 80181, 1980.

3. Anderson, Melvin S.; Stroud, W. Jefferson; Durling, Barbara J.; and Hennessy, Katherine W.: PASCO: Structural Panel Analysis and Sizing Code, Users Manual. NASA TM 80182, 1980.

4. Stroud, W. Jefferson; Greene, William H.; and Anderson, Melvin S.: Buckling Loads for Stiffened Panels Subjected to Combined Longitudinal Compression and Shear Loadings: Results Obtained with PASCO, EAL, and STAGS Computer Programs. NASA TM 83194, 1981.

5. Wittrick, W. H.; and Williams, F. W.: Buckling and Vibration of Anisotropic or Isotropic Plate Assemblies Under Combined Loadings, Int. J. of Mech. Sci., Vol. 16, 1974, pp. 209-239.

6. Vanderplaats, Garret N.: CONMIN - A Fortran Program for Constrained Function Minimization. User's Manual. NASA TM X-62,282, 1973.

7. Vanderplaats, G. N.; and Moses, F.: Structural Optimization by Methods of Feasible Directions. National Symposium on Computerized Structural Analysis and Design, Washington, DC, March 1972.

8. Jones, Robert M.: Mechanics of Composite Materials. Scripta Book Co., 1975.

9. Schmit, Lucien A., Jr.; and Miura, Hirokazu: Approximation Concepts for Efficient Structural Synthesis. NASA CR-2552, 1976.

10. EISI/SPAR Reference Manual, System Level 103, Engineering Information Systems Inc., San Jose, CA, January 1979.

11. Whetstone, W. D.: Engineering Data Management and Structure of Program Functions in New Techniques in Structural Analysis by Computer (Compiled by R. J. Melosh and M. Salana) ASCE Preprint 3601, ASCE Convention and Exposition, Boston, Massachusetts, 1979.

12. Gallagher, Richard H.: Finite Element Analysis, Fundamentals. Prentice-Hall, 1975.

13. Starnes, James H., Jr.; and Haftka, Raphael T.: Preliminary Design of Composite Wing Box Structures For Global Damage Tolerance. Proceedings of AIAA/ASME/ASCE/AHS 21st Structures, Structural Dynamics, and Materials Conference, Seattle, WA, May 12-14, 1980, pp. 529-538.

TABLE I.- LAMINA PROPERTIES OF GRAPHITE-EPOXY MATERIAL USED IN CALCULATIONS

Symbol	Value in SI Units	Value in US Customary Units
E_1	131.0 GPa	19.0×10^6 psi
E_2	13.0 GPa	1.89×10^6 psi
G_{12}	6.41 GPa	$.93 \times 10^6$ psi
μ_1	.38	.38
α_1	$-.378 \times 10^{-6}$ 1/°K	$-.21 \times 10^{-6}$ 1/°F
α_2	28.8×10^{-6} 1/°K	16×10^{-6} 1/°F
ρ	1581 kg/m^3	0.0571 lbm/in^3

TABLE II.- WALL CONSTRUCTION FOR EACH PLATE ELEMENT IN EXAMPLE 1

Layer number starting with outside layer	Thickness		Fiber orientation, deg
	cm	in.	
Plate elements 1 and 3			
1	0.01397	0.00550	45
2	.01397	.00550	-45
3	.01397	.00550	-45
4	.01397	.00550	45
5	.01397	.00550	0
6	.12573	.04950	90
Plate element 2			
1	0.01397	0.00550	45
2	.01397	.00550	-45
3	.01397	.00550	-45
4	.01397	.00550	45
5	.02794	.01100	0

TABLE III.- BUCKLING LOADS FOR EXAMPLE 1

Loading, kN/m		Factor			
		VIPASA		Ortho. plate	EAL
N_x	N_{xy}	$\lambda = L$	$\lambda = L/2$		
0	175.1	0.5721	1.6641	1.4683	1.5525
35.0	175.1	.5353	1.5614	1.3098	1.3985
87.6	175.1	.4862	1.4248	1.1222	1.2060
175.1	175.1	.4182	1.2357	.8222	.8397
350.3	175.1	.3200		.4690	.4764
175.1	0	1.0005		.9970	1.0030

TABLE IV.- WALL CONSTRUCTION FOR EACH PLATE ELEMENT IN EXAMPLE 2

Layer number starting with outside layer	Thickness		Fiber orientation, deg
	cm	in.	
Plate elements 1 and 3			
1	0.01618	0.00637	45
2	.01618	.00637	-45
3	.01618	.00637	-45
4	.01618	.00637	45
5	.06325	.02490	0
6	.10566	.04160	90
Plate element 2			
1	0.02090	0.00823	45
2	.02090	.00823	-45
3	.02090	.00823	-45
4	.02090	.00823	45
5	.17145	.06750	0

TABLE V.- BUCKLING LOADS FOR EXAMPLE 2

Loading, kN/m		Factor			
		VIPASA		Ortho. plate	EAL
N_x	N_{xy}	$\lambda = L$	$\lambda = L/2$		
0	175.1	2.9225	6.6998	9.2435	6.4424
87.6	175.1	2.6742	6.0385	8.0628	5.753
175.1	175.1	2.4574	5.4654	6.7945	5.1630
350.3	175.1	2.0997	4.5367	4.8627	4.12[illegible]
700.5	175.1	1.5964		2.6424	2.[illegible]
175.1	0	9.9724		10.7300	10.[illegible]

TABLE VI.- MASS INDEX AND RATIO OF BUCKLING LOAD TO DESIGN LOAD FOR FIVE GRAPHITE-EPOXY PANELS DESIGNED FOR SEVERAL COMBINATIONS OF LOAD CONDITIONS

Design load conditions	$\frac{W/A}{L}$, kg/m^3	Ratio of lowest buckling load to design load for the following load conditions				
		1	2	3	4	5
1	2.610	1.00	0.05	0.05	0.05	0.13
1,2	4.132	1.00	1.00	.98	.87	.77
1-3	4.158	1.00	1.00	1.00	.88	.77
1-4	4.297	1.07	1.00	1.00	1.00	.95
1-5	4.325	1.04	1.00	1.00	1.00	1.00

TABLE VII.- WALL CONSTRUCTION FOR EACH PLATE ELEMENT IN GRAPHITE-EPOXY PANEL DESIGNED FOR LOAD CONDITIONS 1 TO 5

Layer number starting with outside layer	Thickness		Fiber orientation, deg
	cm	in.	
Plate elements 1 and 3			
1	0.01411	0.005555	45
2	.01411	.005555	-45
3	.01411	.005555	-45
4	.01411	.005555	45
Plate element 2			
1	0.00214	0.000842	45
2	.00214	.000842	-45
3	.00214	.000842	-45
4	.00214	.000842	45
5	.17679	.069604	0

TABLE VIII.- PROPERTIES OF ALUMINUM USED IN EXAMPLE CALCULATIONS

Symbol	Value in SI Units	Value in US Customary Units
E	68.9 GPa	10×10^6 psi
G	26.2 GPa	3.8×10^6 psi
μ	.33	.33
α	23.4×10^{-6} 1/°K	13×10^{-6} 1/°F
ρ	2712 kg/m^3	0.098 lbm/in^3

TABLE IX.- MASS INDEX AND RATIO OF BUCKLING LOAD TO DESIGN LOAD FOR THREE ALUMINUM PANELS DESIGNED FOR SEVERAL COMBINATIONS OF LOAD CONDITIONS

Design load conditions	$\frac{W/A}{L}$, kg/m^3	Ratio of lowest buckling load to design load for the following load conditions		
		1	2	4
1	8.866	1.00	0.86	0.27
1,2	9.158	1.00	1.00	.20
1,2,4	10.569	1.42	1.00	1.00